World Journal of Environmental Biosciences
Available Online at: **www.environmentaljournals.org**

Volume 15, Issue 1: 132-144

https://doi.org/10.51847/ebdOngEMzN

ISSN 2277- 8047

Reclamation of Oil-Polluted Soils with Modified Humic Preparations

Ainash Nauanova[1,2], Zhanar Kassenova[3]*, Maira Kazankapova[3], Bolat Yermagambet[3], Nurgul Kazangapova[1], Ainagul Malgazhdarova[3], Gulnar Nurgazina[4]

[1]Saken Seifullin Kazakh Agrotechnical University, Astana, Kazakhstan.
[2]LLP «BIO-KATU», Astana, Kazakhstan.
[3]«Institute of Coal Chemistry and Technology» LLP, Astana, Kazakhstan.
[4]Astana International University, Astana, Kazakhstan.

ABSTRACT

Soil contamination with oil products remains a pressing environmental issue, particularly in regions with extensive oil production. Promising approaches to remediating such soils include the use of humic substances, which bind pollutants and promote microbiological degradation. This study aimed to evaluate the effectiveness of oil-contaminated soil remediation using basic potassium humate and its modified forms at concentrations of 1% and 10% over a 60-day experimental period. Oil-contaminated soil collected at the "Zhetybai" oil field (Mangistau region, Kazakhstan) was used as the study object. The following humate formulations were used in the experiments: humic acid (1% and 10%), basic potassium humate (1% and 10%), potassium humate modified with silicon (Si), calcium (Ca), magnesium (Mg), and a macronutrient complex (NPK) in the same concentrations. A total of 12 test samples and a control without additives were studied. Oil product concentrations were determined on days 5, 10, 20, 30, and 60. Structural changes were assessed using Fourier transform infrared spectroscopy. The highest purification rates by day 60 were demonstrated by basic potassium humate 10% (77.12%), potassium humate + NPK 10% (74.69%), and potassium humate + Si 10% (68.68%). The modified forms were found to enhance both sorption and biological mechanisms of hydrocarbon degradation. IR spectra confirmed the destruction of oil components and the restoration of humus structures. Humic preparations, especially in combination with nutrient and structure-forming components, are an effective means for accelerated bioremediation of oil-contaminated soils. These findings demonstrate strong potential for field-scale application in the remediation of petroleum-contaminated arid soils.

Keywords: *Humic preparations, Humus, Modification, Petroleum products, Reclamation, Soil*

Corresponding author: Zhanar Kassenova
e-mail ✉ zhanar_k_68@mail.ru
Received: 05 January 2026
Accepted: 02 April 2026

INTRODUCTION

Oil production and refining are critical to the national economy but impose significant environmental burdens, particularly soil degradation caused by spills, pipeline ruptures, and blowouts (Trofimov *et al*., 2023; Svensson & Lindberg, 2026). Petroleum pollutants alter soil physicochemical properties, reduce fertility, and contaminate the atmosphere and groundwater; therefore, biological restoration methods, including humic substances, are increasingly important for soil detoxification and recovery (Vasilyeva *et al*., 2022; Hao *et al*., 2025). Oil contamination generally progresses through surface accumulation, vertical infiltration, and lateral subsurface migration (Cook *et al*., 2002). Effective reclamation consequently combines a technical stage of physical soil management with biological treatment using organic amendments and fertilizers to restore microbial activity and productive capacity (Holliger *et al*., 1997; Kondrashina *et al*., 2018; Shadrin *et al*., 2020).

Humic substances are natural organic complexes, including humic acids, fulvic acids, and humin, that can be obtained from sources such as lignite (Viruel *et al*., 2011; Vaccari *et al*., 2019; Manucharova *et al*., 2021; Morgan *et al*., 2025). Their high sorption and ion-exchange capacities enable the binding of hydrocarbons and heavy metals, while their stimulation of indigenous microorganisms promotes pollutant degradation and beneficial soil microflora (Clarholm *et al*., 2015; Cong *et al*., 2020; Di Fiore *et al*., 2024; Mishra *et al*., 2025). Humic substances also improve soil structure by promoting water-stable aggregation, increasing macroporosity, reducing compaction, and regulating the soil water-air regime (Nagesh *et al*., 2025; Kassenova *et al*., 2025). Accordingly, they may be applied directly, combined with microorganisms, or used as biological fertilizers in contaminated soils (Santos *et al*., 2011; Damaševičius *et al*., 2025).

The remediation effect of humic substances is based on both physicochemical interactions with pollutants and the restoration of soil structure (Yang & Antonietti, 2020; Kassenova *et al*., 2024; Kowalski *et al*., 2024). By promoting stable aggregates and porous soil structures, they improve water retention, aeration, and resistance to compaction (Yang *et al*., 2019; Novak & Dvorak, 2025), as illustrated in **Figure 1**.

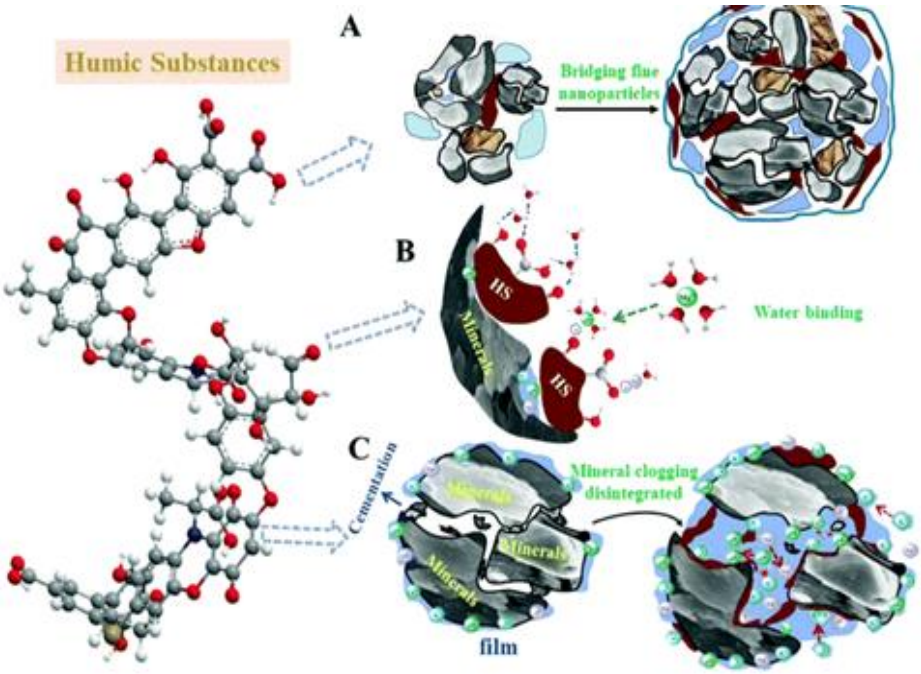

Figure 1. Schematic representation of the influence of humic substances on the physicochemical properties of soil (A: soil structure; B: water-holding capacity; C: cation exchange capacity)

Humic substances also interact with heavy metals through complexation, ion exchange, physical adsorption, and redox reactions **(Figure 2)**. Metal-humic complexes are formed mainly through carboxyl (–COOH) and phenolic (–OH) groups; stronger complexation has been reported for Pb and Cu than for Cd, Zn, and Ni under acidic to moderately acidic conditions (Yang *et al*., 2021; Huber *et al*., 2025).

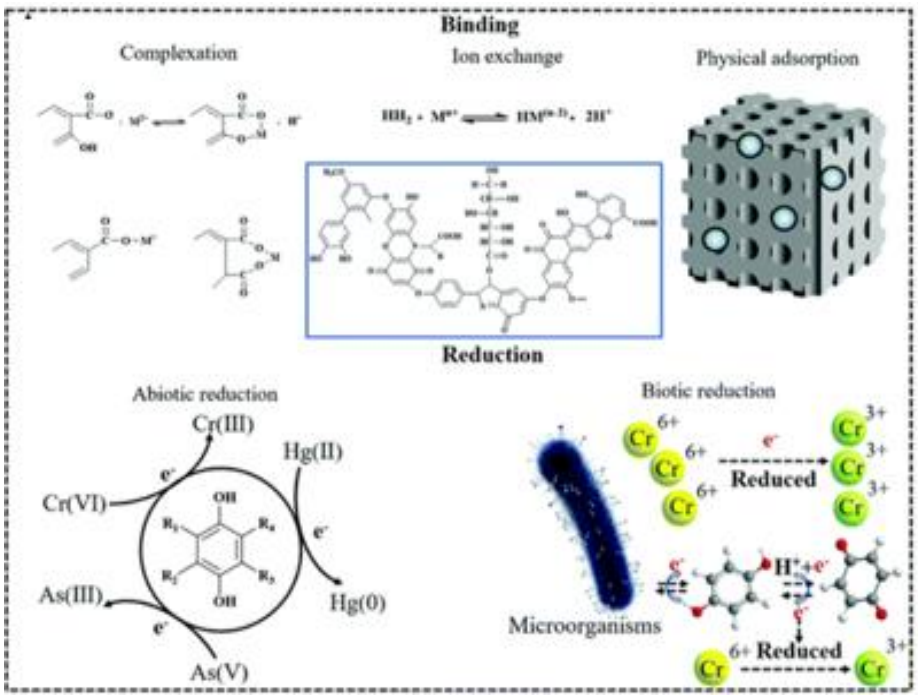

Figure 2. Mechanism of interaction of humic substances with heavy metal ions

Due to their polycarboxylic nature, humic substances adsorb strongly onto aluminum and iron oxides and can modify mineral surface charge, metal bridging, water-holding capacity, and compound solubility (Huang *et al*., 2016; Salem *et al*., 2025). They also influence iron availability. Although soil iron occurs mainly as Fe(III) (Farley *et al*., 2004; Xu *et al*., 2013; Li *et al*.,

2019; Novak & Jelic, 2025), humic substances can promote its conversion to the more plant-available Fe(II), including through photocatalytic and redox processes involving their chromophoric groups (Dobbss *et al*., 2007; Olaetxea *et al*., 2018; Zhu *et al*., 2018; Kajanova & Badrov, 2024) **(Figure 3)**.

Figure 3. Increases in Fe (II) content include the redox properties of humic substances and their participation as a medium for redox reactions under anaerobic conditions

Thus, humic substances can simultaneously promote microbiological and chemical degradation of petroleum components, stabilize metals and other pollutants, reduce their toxicity, and support the restoration of soil fertility (Mora *et al*., 2014; Kwatra *et al*., 2024).

This work aims to evaluate the remediation performance of different modified humic-acid formulations in petroleum-contaminated soils and identify the optimal formulations and treatment conditions. Different concentrations and mineral modifications were examined to determine the most effective preparations for accelerated soil restoration.

MATERIALS AND METHODS

A laboratory-scale experimental study was conducted to evaluate the effectiveness of humic preparations for the remediation of oil-contaminated soils from arid regions of Kazakhstan. The experiment included the analysis of untreated oil-contaminated soil, soil treated with basic potassium humate, and soil treated with various modified forms of potassium humate.

All experimental investigations were carried out under controlled laboratory conditions during a single incubation cycle following the simultaneous application of all treatment variants. The objective of the study was to assess the efficiency of petroleum-contaminated soil remediation using potassium humate and its modified forms and to identify the most effective compositions and treatment conditions.

Sampling and preparation of humic preparations

Oil-contaminated soil samples were collected from the Zhetybai oil field (Mangistau region, Republic of Kazakhstan) in areas with visually confirmed petroleum contamination. Sampling was performed under dry weather conditions from the topsoil layer (0–20 cm). Composite samples were prepared by combining several point samples, and at least three independent composite samples were obtained. Before the experiment, soils were cleared of plant residues and stored in sealed containers at room temperature.

Potassium humate was obtained from oxidized brown coal from the Sarykol deposit (Republic of Kazakhstan), preground to a particle size of less than 0.5 mm. The coal characteristics (wt.%) were as follows: A^d - 66.09; W^r - 5.73; V^d - 17.78; S^{td} - 0.71; C^{td} - 21,01; H^{td} - 1,68; N^{td} - 2.09; Na - 0.61; Al - 0.89; K - 0.58; Ca - 0.31; Ti - 0.22; Fe - 1.11; Zr - 0.08. The particle size distribution was 2.95 μm (10%), 63.8 μm (50%), and 452 μm (90%).

Humic preparations were produced using a rotary-pulsation apparatus and an ultrasonic reactor with an air supply, promoting coal oxidation and increasing the yield of humic substances. The particle size after treatment ranged from 19.2 nm to 3.57 μm. The process temperature did not exceed 50–55 °C, which is suitable for oxidation by atmospheric oxygen and extraction of humic and fulvic acid salts. As a result, a finely dispersed humic system with submicron particles was formed using cavitation dispersion based on electrophysical action.

For different experimental variants, humic preparations were obtained by stirring the solutions on an IKA RH basic 2 magnetic stirrer for 30 min, followed by ultrasonic treatment in a GRAD ultrasonic bath for 30 min at 55 °C and subsequent cooling (Yermagambet *et al*., 2021)

Laboratory experiment

The experiment included thirteen variants, including a control (untreated contaminated soil). Experimental treatments

involved soil amendment with potassium humate solutions at concentrations of 1% and 10%, as well as modified forms containing Si, NPK, Ca, Mg, and humic acid. Each treatment was performed in triplicate.

Soil treatment was carried out by uniform application of the corresponding solutions, followed by thorough mixing. Incubation was conducted at 20–25 °C with soil moisture maintained at 60–70% of field capacity. Aeration was ensured by periodic loosening. Indigenous microbiological activity was not suppressed.

In addition to the soil treatment experiments, FTIR analysis was performed for a model humic organomineral system. The commercial humic organomineral fertilizer "Kazuglegumus" was combined with activated aluminum alloy at a mass ratio of 1:1. This system was not applied directly to soil but was analyzed separately to investigate the nature of interactions between humic substances and mineral components. FTIR spectra were recorded to identify functional groups involved in humic–metal complex formation and to support the interpretation of the soil treatment results (Taran *et al*., 2013; Akhanova *et al*., 2023).

Analytical methods

Elemental analysis of soil samples was performed using the Pregl–Dumas method. Humus content was determined according to GOST 26213–2021 (Federal Agency for Technical Regulation and Metrology, 2021), and soil pH was measured following GOST 26483–85 (State Committee of the USSR for Standards, 1985; Abdoul-Latif *et al*., 2025). The mass fraction of petroleum products was determined by a gravimetric method in accordance with RD 52.18.647–2003.

Functional group composition of soil organic matter and humic compounds was analyzed by Fourier-transform infrared (FTIR) spectroscopy using an ALPHA II QuickSnap spectrometer. Heavy metal concentrations were determined by atomic absorption spectrometry (AAS) using a Shimadzu AA-7000 instrument (Kuzyakov *et al*., 1990; Zairkhanova *et al*., 2024).

Statistical analysis

Statistical analysis was performed using standard methods. Results are presented as mean ± standard deviation (M ± SD). Differences between treatments were evaluated using analysis of variance (ANOVA) at a significance level of $p < 0.05$. Post hoc comparisons were conducted using Tukey's HSD test.

RESULTS AND DISCUSSION

The soil reaction remained near neutral across all experimental variants, with pH values ranging from 7.10 to 7.32. The untreated oil-contaminated soil had a pH of 7.32 and a humus content of 7.49%. In soils treated with 1 and 10% basic potassium humate, the pH values were 7.29 and 7.20, while the humus contents increased to 9.77 and 9.51%, respectively. The application of potassium humate modified with Si resulted in pH values of 7.30 and 7.18 and humus contents of 8.35 and 8.71% at concentrations of 1 and 10%, respectively. The NPK-modified variants had pH values of 7.28 and 7.10 and the lowest humus contents, amounting to 6.09 and 5.96%. In soils treated with potassium humate modified with Ca, the pH values were 7.31 and 7.24, and the humus contents were 7.30 and 6.69%. The Mg-modified variants showed pH values of 7.28 and 7.16 and humus contents of 7.96 and 8.33%. Humic acid at concentrations of 1 and 10% resulted in pH values of 7.29 and 7.22 and humus contents of 9.05 and 11.42%, respectively. Thus, the highest humus content was recorded after the application of 10% humic acid, whereas the NPK-modified treatments were associated with the lowest humus values.

The mass fraction of petroleum products was determined on days 5, 10, 20, 30, and 60 of incubation. The initial petroleum product content in the untreated oil-contaminated soil was 86,528 ± 1,200 mg/kg, and no purification was observed in the control. After five days, the petroleum product concentrations in the treated samples remained relatively high, ranging from 72,000 to 87,450 mg/kg. A gradual decline was subsequently recorded, with concentrations ranging from 69,000 to 81,500 mg/kg on day 10, from 62,500 to 78,000 mg/kg on day 20, from 61,800 to 74,200 mg/kg on day 30, and from 19,800 to 54,300 mg/kg on day 60.

The highest remediation efficiency was achieved with 10% basic potassium humate, which reduced the petroleum product content to 19,800 ± 540 mg/kg and provided 77.12% purification. This treatment was followed by potassium humate + NPK at 10%, with a residual concentration of 21,900 ± 540 mg/kg and 74.69% purification, and potassium humate + NPK at 1%, with 24,400 ± 610 mg/kg and 71.80% purification. Potassium humate + Si at 10% reduced the contaminant content to 27,100 ± 690 mg/kg, corresponding to 68.68% purification, while 1% basic potassium humate and 1% potassium humate + Si provided purification efficiencies of 67.18 and 64.17%, respectively.

The Ca-modified formulations demonstrated moderate effectiveness, with purification efficiencies of 57.24% at 1% and 55.51% at 10%. Similar results were obtained for the Mg-modified formulations, which provided 54.93 and 56.78% purification. Humic acid was less effective than potassium humate and its modified forms: the residual petroleum product concentrations were 54,300 ± 980 mg/kg at 1% and 41,400 ± 850 mg/kg at 10%, corresponding to purification efficiencies of 37.25 and 52.15%, respectively. Statistical analysis performed separately for each sampling date demonstrated significant treatment-related differences at $p < 0.05$.

Analysis of the data obtained indicates a significant decrease in the mass fraction of petroleum products (PP) in the soil when using various forms of humic substances and their modified compositions. The initial concentration of PP in the contaminated soil was 86 528 mg/kg. During the experiment, a gradual decrease in the content of PP in samples treated with various humate compositions was observed for 60 days.

All experimental data are expressed as mean values with corresponding standard deviations (mean ± SD) obtained from replicate measurements. Statistical analysis was performed separately for each sampling time (5, 10, 20, 30, and 60 days). The significance of differences between the treatments was evaluated using one-way analysis of variance (ANOVA). When statistically significant differences were detected, the means were further compared using Tukey's honest significant difference (HSD) post hoc test. Superscript lowercase letters (a–f) indicate the results of the multiple comparison analysis: values marked with different letters within the same column differ significantly from each other at a confidence level of 95%

($p < 0.05$), whereas values sharing at least one identical letter do not show statistically significant differences.

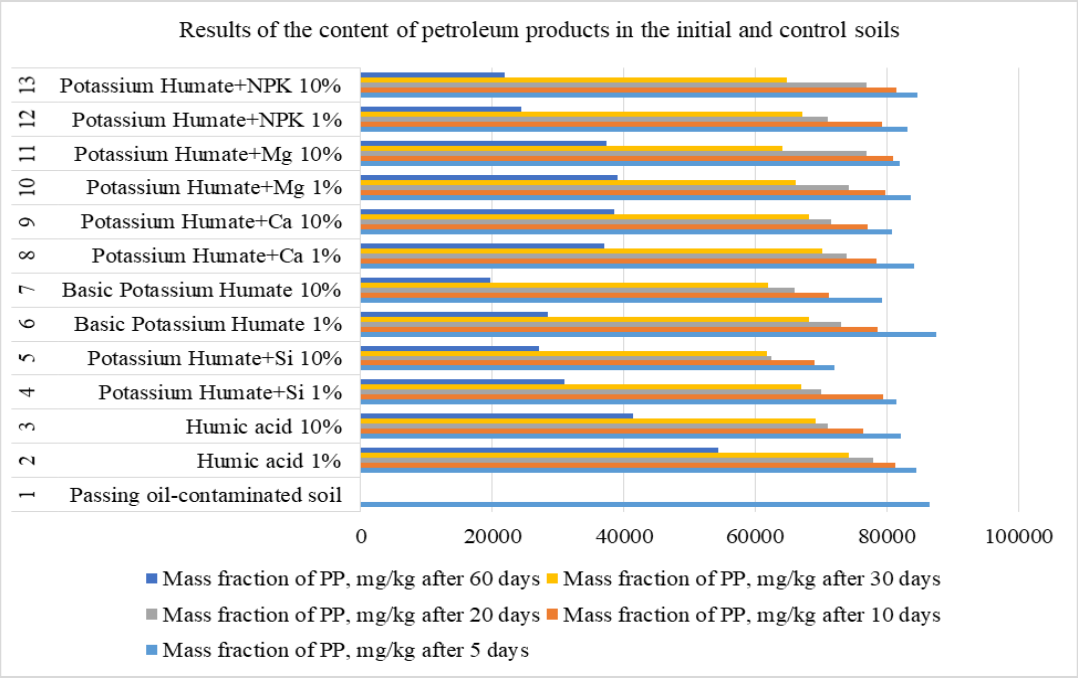

Figure 4. The content of the mass fraction of petroleum products in soils

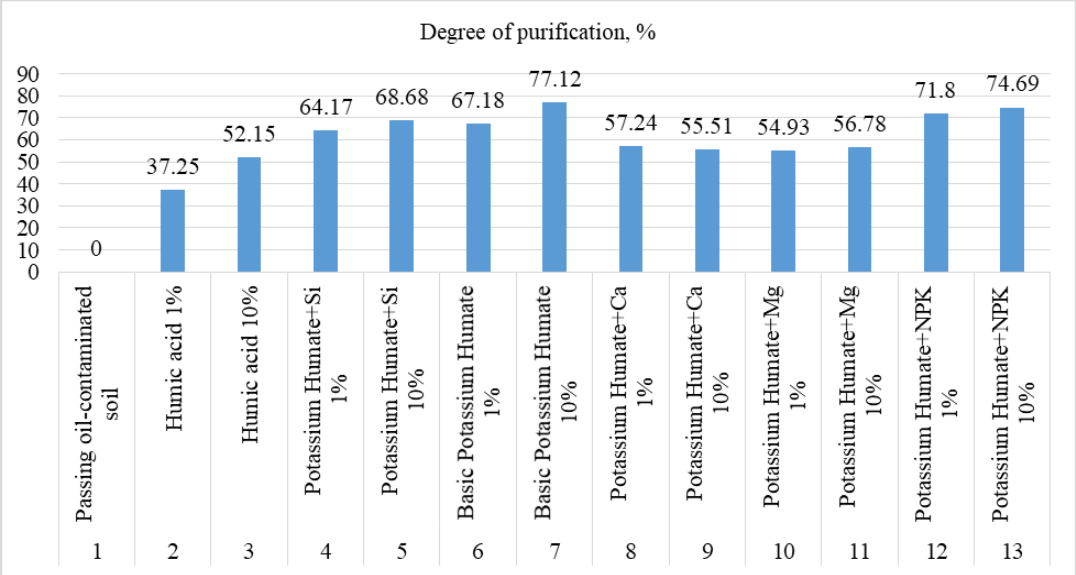

Figure 5. Determination of the degree of soil purification depending on the modification

Heavy metals play an important role in the processes of contamination and subsequent analysis of petroleum products in the soil. In oil pollution conditions, they can form stable complexes with organic petroleum compounds, changing the physico-chemical properties of the soil system and complicating the extraction process of petroleum products. This, in turn, may affect the accuracy of determining their mass fraction.

The use of humic substances in such systems not only contributes to the decomposition and leaching of petroleum products, but also has a sorption and complexing effect on heavy metals. Humic acids are able to bind metal ions (for example, Pb^{2+}, Cd^{2+}, Cu^{2+}, Zn^{2+}), reducing their mobility and toxicity. Thus, humic preparations not only improve the degradation of petroleum products but also reduce the interfering effect of heavy metals in their analytical determination, contributing to a more accurate assessment of the degree of contamination and the effectiveness of remediation. **Table 1** below shows the

results of determining the content of heavy metals in the initial and treated soil.

Table 1. Content of mass concentration of heavy metals in the soil before and after treatment with humic substances

No.	Name of the sample	Cd	Pb	Zn	As
	Initial sample of oil-contaminated soil (without treatment)				
1	Passing oil-contaminated soil	Not detected	Not detected	36.66	4.16
	Oil-contaminated soil treated with humic preparations.				
2	Humic acid 1%	Not detected	Not detected	34.76	Not detected
3	Humic acid 10%	Not detected	Not detected	33.76	2.58
4	Potassium Humate+Si 1%	Not detected	Not detected	37.00	6.25
5	Potassium Humate+Si 10%	Not detected	Not detected	33.00	6.12
6	Basic Potassium Humate 1%	Not detected	Not detected	30.00	10.80
7	Basic Potassium Humate 10%	Not detected	Not detected	27.00	6.20
8	Potassium Humate+Ca 1%	Not detected	Not detected	24.45	Not detected
9	Potassium Humate+Ca 10%	Not detected	Not detected	34.76	Not detected
10	Potassium Humate+Mg 1%	Not detected	Not detected	30.44	2.58
11	Potassium Humate+Mg 10%	Not detected	Not detected	33.76	Not detected
12	Potassium Humate+NPK 1%	Not detected	Not detected	Not detected	9.35
13	Potassium Humate+NPK 10%	Not detected	Not detected	33.39	3.00
14	Permissible limit (maximum permissible concentration, etc.)	0.5-1	6.00	23.00	4.16

The spectral data obtained from the studied soils are presented in **Table 2**, providing a comparative overview of the key vibrational features identified in each treatment scenario.

Table 2. IR spectra of the obtained samples

No.	Name of samples	Interpretation
1	Passing oil-contaminated soil 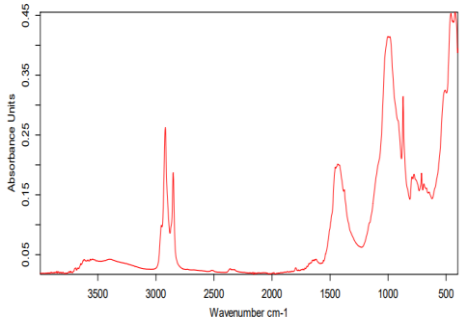	3500–3200 cm^{-1} — O–H (hydrogen-bonded hydroxyls, water, phenols) 2950–2850 cm^{-1} — C–H (alphatic CH_2/CH_3, petroleum hydrocarbons) 1700–1500 cm^{-1} — C=O, C=C, COO^-, amides (organics; oxy- and aromatic structures) 1300–1000 cm^{-1} — C–O, Si–O, polysaccharides, silica <1000 cm^{-1} — "mineral" region: silica, carbonates, aromas (out-of-plane C–H vibrations).
2	Potassium Humate+Si 1% 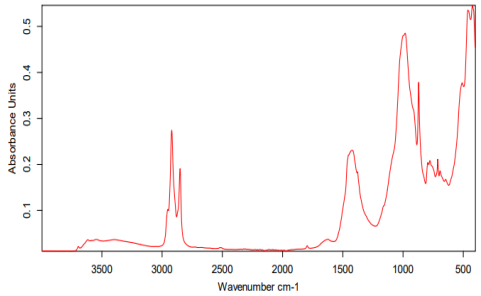	3542 cm^{-1} – stretching vibrations of –OH groups (hydroxyl, humic substances, adsorbed water). 2919 and 2850 cm^{-1} – stretching vibrations of C–H in $–CH_2$ and $–CH_3$ groups (hydrocarbons, oil residues, humus). 1417 cm^{-1} – deformation vibrations of C–H may also indicate the presence of carbonates. 982 cm^{-1} – vibrations of Si–O (quartz, clay minerals). 870 cm^{-1} – deformation vibrations of carbonates (CO_3^{2-}). 776 cm^{-1} – vibrations of quartz, silica. 712 and 692 cm^{-1} – stretching vibrations of carbonate groups. 509 cm^{-1} – Si–O–Si vibrations (clay minerals, silicate matrix). 461 and 424 cm^{-1} – deformation vibrations of silica and minerals.
3	Potassium Humate+Si 10%	3399 cm^{-1} – broad –OH absorption (hydroxyl groups of humic substances, bound water). 2919 and 2850 cm^{-1} – C–H oscillations $–CH_2$ and $–CH_3$ (hydrocarbons, petroleum residues). 1415 cm^{-1} – C–H deformation oscillations or carbonate groups (CO_3^{2-}). 981 cm^{-1} – Si–O oscillations (clay minerals, quartz).

	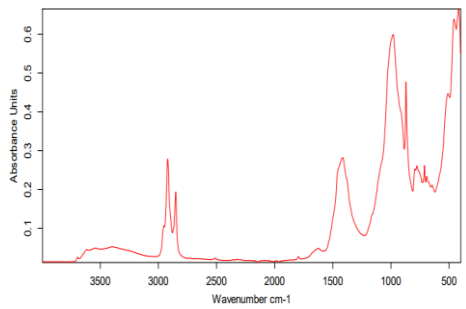	870 cm^{-1} – carbonate groups (CO_3^{2-} deformations). 776 cm^{-1} – quartz, silica. 711 and 692 cm^{-1} – carbonates (characteristic calcite/dolomite bands). 509 cm^{-1} – Si–O–Si vibrations (silicates, clay minerals). 458 and 419 cm^{-1} – deformation vibrations of silica and minerals.
4	Basic Potassium Humate 1% 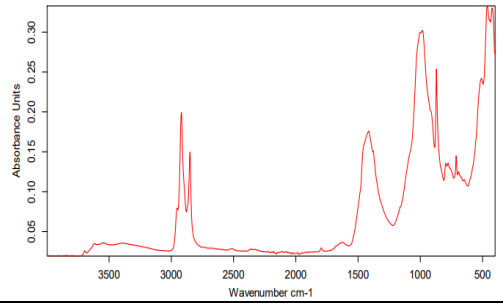	3547 cm^{-1} – OH stretching vibrations (hydroxyl groups, humus, water). 2918 and 2850 cm^{-1} – C–H vibrations $–CH_2$, $–CH_3$ (oil hydrocarbon residues, organic matter). 1416 cm^{-1} – C–H deformation vibrations and/or carbonate groups. 982 cm^{-1} – Si–O vibrations (clay minerals, quartz). 870 cm^{-1} – carbonates (characteristic CO_3^{2-} peak). 777 cm^{-1} – quartz, silica. 711 cm^{-1} – carbonate vibrations (calcite/dolomite). 509 cm^{-1} – Si–O–Si (clay minerals, silicate matrix). 462 and 423 cm^{-1} – deformation vibrations of silica and silicates.
5	Basic Potassium Humate 10% 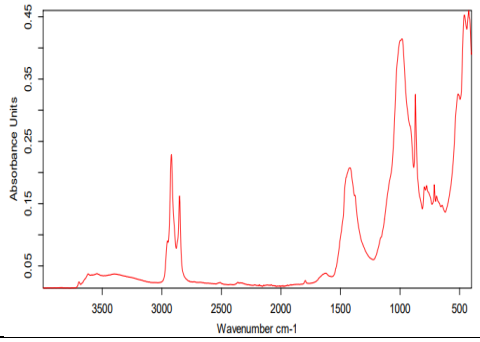	3543 cm^{-1} – –OH stretching vibrations (humic substances, water, hydroxyl groups of minerals). 2920 and 2851 cm^{-1} – C–H vibrations $–CH_2$ and $–CH_3$ (hydrocarbon fragments, oil residues). 1418 cm^{-1} – C–H deformation vibrations and/or the presence of carbonates (CO_3^{2-}). 983 cm^{-1} – Si–O vibrations (clay minerals, quartz). 870 cm^{-1} – deformations of carbonate groups (typical of calcite). 776 cm^{-1} – quartz, silica. 711 and 692 cm^{-1} – carbonate vibrations (calcite/dolomite). 512 cm^{-1} – Si–O–Si bonds (clay minerals, silicate matrix). 459 and 423 cm^{-1} – deformation vibrations of silica and minerals.
6	Potassium Humate+Ca 1% 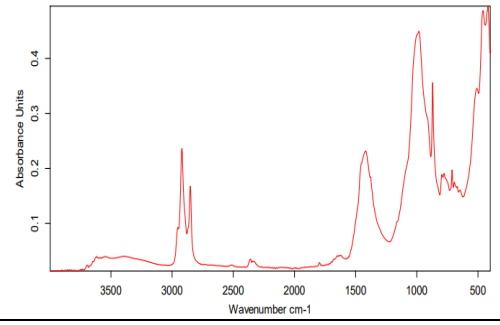	3392 cm^{-1} – –OH stretching vibrations (humus, water, hydroxyl groups of minerals). 2919 and 2850 cm^{-1} – C–H vibrations $–CH_2$/$–CH_3$ (hydrocarbons, organics). 2360 cm^{-1} – associated with CO_2 vibrations (adsorbed carbon dioxide, carbonates). 1417 cm^{-1} – C–H deformation vibrations, possible carbonates (CO_3^{2-}). 982 cm^{-1} – Si–O vibrations (clay minerals, quartz). 870 cm^{-1} – characteristic peak of carbonates (calcite). 777 cm^{-1} – quartz, silica. 711 and 692 cm^{-1} – carbonate groups (calcite/dolomite). 510 cm^{-1} – Si–O–Si bonds (silicates, clays).
7	Potassium Humate+Ca 10% 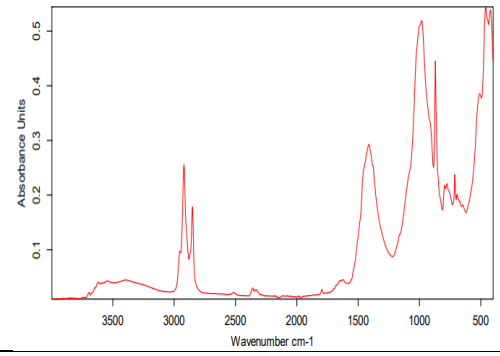	3399 cm^{-1} – OH stretching vibrations (humic substances, water, hydroxyl groups of minerals). 2919 and 2850 cm^{-1} – C–H vibrations of $–CH_2$ and $–CH_3$ (hydrocarbons, organic matter, petroleum residues). 2359 cm^{-1} – CO_2 band (adsorbed carbon dioxide, carbonates). 1412 cm^{-1} – C–H deformation vibrations and/or carbonate groups (CO_3^{2-}). 982 cm^{-1} – Si–O vibrations (clay minerals, quartz). 870 cm^{-1} – carbonates (calcite, dolomite). 777 cm^{-1} – quartz, silica. 711 and 693 cm^{-1} – carbonate groups (characteristic peaks of calcite/dolomite). 509 cm^{-1} – Si–O–Si (silicates, clay minerals).
8	Potassium Humate+Mg 1%	3399 cm^{-1} – O–H stretching (hydroxyl groups, water/alcohols, surface –OH).

	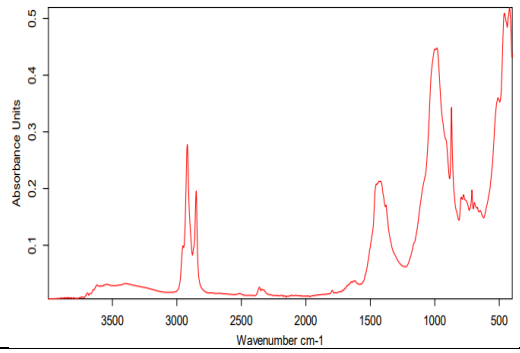	2919 and 2850 cm^{-1} – C–H stretching vibrations (–CH_2, –CH_3). 2360 cm^{-1} – traces of CO_2 or adsorbed gases. 1418 cm^{-1} – C–H deformation vibrations (–CH_2/–CH_3). 983 cm^{-1} – possible C–O vibrations or C–H out-of-plane deformations. 870 cm^{-1} – C–H deformation vibrations (aromatic or vinylic). 777 and 712 cm^{-1} – "fingerprint" of the aromatic ring (characteristic peaks of the benzene ring). 692 cm^{-1} is also an aromatic system, an indicator of mono- or para-substituted rings. 460 and 420 cm^{-1} are low-frequency vibrations (metal-oxygen bonds, minerals, lattice deformations).
9	Potassium Humate+Mg 10% 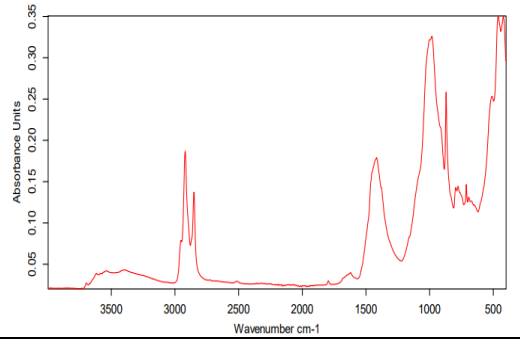	3402 cm^{-1} – O–H stretching (hydroxyl groups, sorbed water/alcohols). 2920 and 2851 cm^{-1} – C–H stretching (–CH_2, –CH_3). 1622 cm^{-1} – C=C stretching vibrations (aromatic rings) or H–O–H bending vibrations of water. 1417 cm^{-1} – C–H bending vibrations (–CH_2/–CH_3). 983 cm^{-1} – C–O vibrations / C–H bending (out-of-plane). 870 cm^{-1} – aromatic or vinylic C–H bending. 777, 712, and 693 cm^{-1} – aromatic ring imprint (characteristic of benzene structures, para-substitution). 511, 461, and 422 cm^{-1} – low-frequency vibrations (lattice, metal–O bonds, mineral impurities).
10	Potassium Humate+NPK 1% 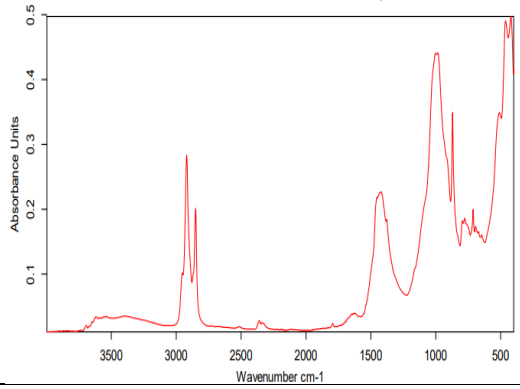	3401 cm^{-1} — broad O–H band: hydroxyl groups (humus, phenols), bound water, surface –OH groups of minerals. 2919 and 2850 cm^{-1} — C–H stretching vibrations (–CH_2, –CH_3): saturated alkane fragments — oil/fat residues. 2360 cm^{-1} — CO_2 signal (adsorbed carbon dioxide or carbonate adsorbates). 1419 cm^{-1} — C–H deformation vibrations and/or carbonate components (CO_3^{2-}). 983–984 cm^{-1} — Si–O / C–O vibrations: quartz, silicates, polysaccharide/ester groups of organic matter. 870 cm^{-1} — carbonate deformation (typical of calcite) or out-of-plane C–H vibrations of aromatic systems. 777 cm^{-1} — silica/quartz vibrations (Si–O–Si) or specific mineral bands. 712 and 693 cm^{-1} — out-of-plane C–H vibrations (aromatic systems) and/or carbonate signatures (calcite/dolomite). 510 cm^{-1} — Si–O–Si bending (clay minerals, silicates). 462 and 420 cm^{-1} — low-frequency mineral deformations (silica, clay matrix, metal-oxide bonds).
11	Potassium Humate+NPK 10% 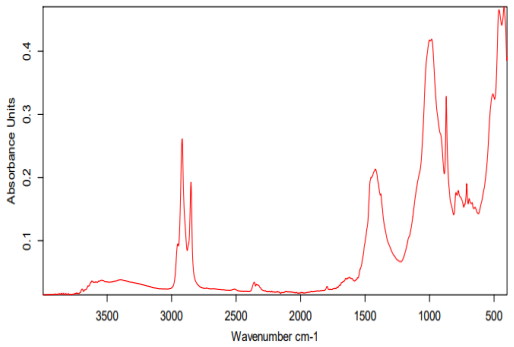	3399 cm^{-1} — broad O–H band: hydroxyl groups (humus, phenols), bound water, surface –OH of minerals. 2918 and 2849 cm^{-1} — C–H stretching vibrations (–CH_2, –CH_3): saturated alkane fragments — oil/fat residues. 2359–2360 cm^{-1} — CO_2 signal (adsorbed carbon dioxide or carbonate adsorbates). 1419 cm^{-1} — C–H deformation vibrations and/or carbonate components (CO_3^{2-}). 984 cm^{-1} — Si–O / C–O vibrations: quartz, silicates, possible polysaccharide C–O groups. 870 cm^{-1} — carbonate deformations (calcite) or out-of-plane vibrations of aromatic C–H. 777 cm^{-1} — silica / Si–O–Si bends (quartz, silicate matrix). 712 and 693 cm^{-1} — out-of-plane C–H vibrations of aromatic rings and/or carbonate signatures (calcite/dolomite). 509 cm^{-1} — Si–O–Si bends (clay minerals, silicates).
12	Humic organomineral fertilizer "Kazuglegumus" + Activated aluminum alloy (weight ratio (1:1))	1577 cm^{-1} — complex absorption band: asymmetric stretching vibrations of COO^- (carboxylate ion), indicating coordination of carboxyl groups in complex compounds. 2116 cm^{-1} — new absorption band: characteristic of complex formation, associated with metal–ligand interactions in aluminum–humic substance complexes. 2100–2400 cm^{-1} — broad absorption region: typical for aluminum complexes with humic substances, reflecting coordination bonds between Al^{3+} ions and functional groups of humic matter.

	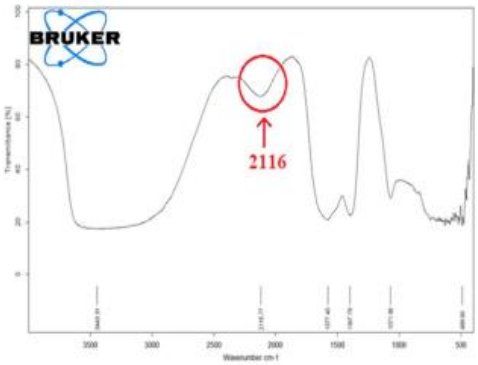	1000–1100 cm^{-1} — deformation O–H vibrations and C–O stretching: phenolic and alcoholic hydroxyl groups, characteristic of humic substances.
13	Humic organomineral fertilizer "Kazuglegumus" + Activated aluminum alloy (weight ratio (1:1)) 1-oil-contaminated soil; 2-oil-free soil; 3-soil after treatment with a complex organomineral reagent 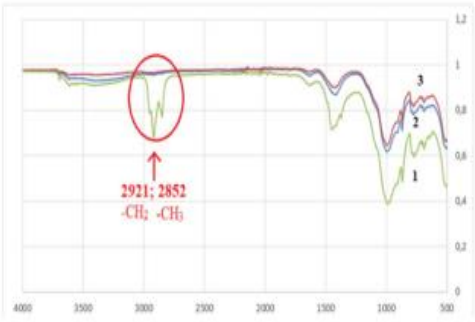	2921 and 2852 cm^{-1} — asymmetric and symmetric C–H stretching vibrations ($–CH_2$, $–CH_3$): aliphatic hydrocarbon fragments, characteristic of oil components. 1453 and 1376 cm^{-1} — deformation vibrations of C–H and C–C bonds: aliphatic hydrocarbons. 900–700 cm^{-1} — out-of-plane C–H bending vibrations: aromatic structures typical of petroleum hydrocarbons. 1428 cm^{-1} — CO_3^{2-} vibration: carbonate groups in mineral components of soil. ~1630 cm^{-1} — bending vibrations of adsorbed water and/or aromatic C=C stretching: decrease in intensity indicates reduction of oil-related organic matter. 999 cm^{-1} — Si–O–Si stretching vibrations: silicate minerals. 780, 688, 533, and 469 cm^{-1} — metal–oxygen vibrations: Mg–O and Al–O bonds in clay and mineral phases.

The maintenance of a near-neutral soil reaction across most treatments indicates the buffering capacity of modified humic preparations. The slight decrease in pH in Mg- and NPK-enriched variants may reflect ion-exchange interactions between macronutrients and functional groups of the organic matrix (Yang *et al*., 2021; Kassenova *et al*., 2024; Nguyen *et al*., 2025), whereas the stability of Si- and Ca-containing treatments suggests maintenance of soil chemical equilibrium during petroleum degradation (Aksoy & Akaydin, 2024; Kassenova *et al*., 2024). Humic acid and potassium humate also increased the stable organic fraction of the soil (Kassenova *et al*., 2024; Elango & Govindaraju, 2025). Silicon and magnesium may further stabilize organic matter through organo-mineral complex formation (Huang *et al*., 2016; Yang *et al*., 2021), while high NPK concentrations can stimulate microbial activity and simultaneously accelerate mineralization of stable soil carbon (Kassenova *et al*., 2024). Therefore, amendment composition should balance enhanced bioremediation with preservation of soil organic matter (Jannath *et al*., 2024; Kassenova *et al*., 2024).

The treatment-dependent changes in arsenic concentrations shown in **Table 1** indicate that humic-based remediation may also influence metalloid mobility. Although humic substances generally immobilize metals such as Cd and Pb through complexation with carboxyl and phenolic groups (Yang *et al*., 2021; Kassenova *et al*., 2024; Chandrasekhar *et al*., 2025), arsenic behavior is more complex because humic substances may compete for adsorption sites on iron and aluminum oxyhydroxides and thereby enhance As mobility (Moreno-Jiménez *et al*., 2011; Xue *et al*., 2019). They can also act as electron shuttles facilitating microbial reduction of As(V) to more mobile forms (Qiao *et al*., 2019). The direction of this effect depends on humic composition: different humic fractions may either stabilize or enhance arsenic migration (Wang *et al*., 2022; Duan *et al*., 2024). Consequently, the application of modified humic preparations in soils with elevated metalloid contents requires monitoring of possible groundwater contamination and plant uptake (Moreno-Jiménez *et al*., 2011; Kondrashina *et al*., 2018; Shadrin *et al*., 2020; Vikram *et al*., 2022; Duan *et al*., 2024).

Petroleum hydrocarbon concentrations changed little during the first five days, whereas a clear reduction became evident from day 10 and was most pronounced between days 10 and 30. By day 60, degradation slowed, probably because readily degradable hydrocarbon fractions had been depleted. The untreated control showed little evidence of effective self-purification, while all humic treatments enhanced petroleum removal. Basic potassium humate at 10% produced the highest purification efficiency (77.12%), followed by NPK-modified humate at 10% (74.69%) and Si-modified humate at 10% (68.68%). Ca- and Mg-modified humates showed moderate effects, whereas humic acid was less effective than potassium humate and its most efficient modifications. Overall, the final performance followed the general order: potassium humate 10% > humate + NPK > humate + Si > Ca- and Mg-modified humates > humic acid > control. The temporal dynamics and final purification efficiencies are presented in **Figures 4 and 5**.

These differences can be attributed to the mechanisms of the additives. Potassium humate can adsorb and emulsify petroleum compounds, increase their bioavailability, bind toxic intermediates, and stimulate hydrocarbon-degrading

microorganisms. NPK additionally compensates for nitrogen and phosphorus limitations, supporting microbial growth and explaining the high performance of NPK-enriched humate. Silicon may improve soil structure, aeration, and hydrocarbon sorption, whereas magnesium supports microbial enzymatic processes. Calcium humate may be less effective because of its lower solubility and mobility, while the comparatively poor solubility of humic acid can delay the release of active fractions. Thus, nutrient and structure-forming modifications can substantially enhance humate-mediated remediation, as demonstrated in **Figures 4 and 5**.

Humic treatments also influenced heavy-metal behavior **(Table 1)**. Zinc concentrations varied among treatments, indicating differences in metal–humate interactions, while arsenic showed greater treatment-dependent variability. Cadmium and lead remained below detection limits in the analyzed samples. These findings support the capacity of humic substances to modify metal mobility but also emphasize the need to consider metalloid behavior when evaluating the environmental safety of remediation.

FTIR results summarized in **Table 2** provide additional evidence of structural changes in treated soils. The spectra retained characteristic bands of hydroxyl groups (3400–3550 cm^{-1}), aliphatic C–H vibrations (2919–2850 cm^{-1}), carbonate and silicate structures (1400–1000 cm^{-1}), and mineral lattice vibrations below 800 cm^{-1}, indicating preservation of the mineral framework. At the same time, potassium humate 10% and the NPK- and Si-modified treatments showed attenuation of hydrocarbon-related bands in the 2920–2850 and 900–700 cm^{-1} regions and near 1630 cm^{-1}, consistent with petroleum degradation or immobilization.

These FTIR changes agree with published data on humic-based organomineral systems (Taran *et al*., 2013; Akhanova *et al*., 2023). The "Kazuglegumus"–activated aluminum system shows carboxylate vibrations at 1577 cm^{-1} and metal–ligand interaction bands near 2116 cm^{-1}, supporting the involvement of carboxyl, phenolic, and hydroxyl groups in the formation of stable humic–mineral complexes (Taran *et al*., 2013; Akhanova *et al*., 2023). Overall, the combined chemical and spectroscopic results indicate that 10% potassium humate and its NPK- and Si-modified forms provide the most effective remediation by promoting hydrocarbon removal while supporting the formation of a stable organomineral matrix (Akhanova *et al*., 2023).

CONCLUSION

The study confirmed the effectiveness of humate preparations for remediating oil-contaminated soil. The highest purification efficiencies were achieved with 10% basic potassium humate (77.12%), potassium humate + NPK (74.69%), and potassium humate + Si (68.68%). FTIR analysis showed a decrease in hydrocarbon-related absorption bands while signals associated with humic and mineral components were retained, indicating both petroleum degradation and preservation of the soil organomineral structure. Overall, potassium humate, particularly when combined with nutrient and structure-forming additives, accelerated hydrocarbon removal and supported restoration of degraded soil properties.

The main limitations are related to the laboratory-scale design, the absence of microbial community analyses, and the lack of a techno-economic assessment. Soil heterogeneity, environmental variability, and mixed contamination may affect treatment performance under field conditions. Future studies should therefore include pilot- and field-scale validation, analysis of microbial diversity and degradation pathways, and engineering and cost–benefit assessments to determine the feasibility of large-scale application.

ACKNOWLEDGMENTS: The authors sincerely thank the Editors and anonymous reviewers for their careful evaluation of the manuscript and for their constructive comments and valuable recommendations, which helped improve the quality and clarity of the paper.

CONFLICT OF INTEREST: None

FINANCIAL SUPPORT: This research has been funded by the Science Committee of the Ministry of Science and Higher Education of the Republic of Kazakhstan (Grant No. BR24992961 "Development of new technologies using biological systems for processing coal waste into organo-mineral fertilizer to increase soil fertility and crop productivity").

ETHICS STATEMENT: None

REFERENCES

Abdoul-Latif, F. M., Ainane, A., Saoudi, O., Mohamed, H., Ali, A. M., Cacciatore, S., & Ainane, T. (2025). Confrontation of the ambivalent roles of the intestinal microbiota in carcinogenesis: Oncogenic or anticancer agents? *Journal of Advanced Pharmacy Education and Research, 15*(2), 16–30. doi:10.51847/XocFRvwLrp

Akhanova, T. R., Lyubchenko, N. P., Sarmurzina, R. G., Karabalin, U. S., Muhr, H., & Boiko, G. I. (2023). Complex restoration of oil-contaminated soils with new organomineral reagents. *Water, Air, & Soil Pollution, 234*(11), 686. doi:10.1007/s11270-023-06689-8

Aksoy, C., & Akaydin, A. (2024). The impact of strategic leadership on employee performance: A study of the aviation industry. *Journal of Organizational Behavior Research, 9*(2), 42–53. doi:10.51847/3xix5orUCJ

Chandrasekhar, K., Nastro, R. A., Narayana, A. V., Rao, A. R., Singh, M., & Chennaiah, A. (2025). Microbial cell factory engineering for scalable production of bio-commodities: Emphasis on robustness. *Journal of Biochemical Technology, 16*(3), 19–29. doi:10.51847/6z0mtOiyyc

Clarholm, M., Skyllberg, U., & Rosling, A. (2015). Organic acid-induced release of nutrients from metal-stabilized soil organic matter–the unbutton model. *Soil Biology and Biochemistry, 84*, 168–176. doi:10.1016/j.soilbio.2015.02.019

Cong, W. F., Suriyagoda, L. D., & Lambers, H. (2020). Tightening the phosphorus cycle through phosphorus-efficient crop genotypes. *Trends in Plant Science, 25*(10), 967–975. doi:10.1016/j.tplants.2020.04.013

Cook, S. V., Chu, A., & Goodman, R. H. (2002). Leachability and toxicity of hydrocarbons, metals, and salt contamination

from flare pit soil. *Water, Air, and Soil Pollution, 133*, 297–314. doi:10.1023/A:1012925812698

Damaševičius, R., Maskeliūnas, R., & Blažauskas, T. (2025). Enhancing virtual medical history taking: Effects of customized guidelines in two serious games for medical education. *Annals of Pharmacy Education, Safety, and Public Health Advocacy, 5*, 39–49. doi:10.51847/kNshKQSf5t

Di Fiore, A., Stellini, E., Savio, G., Rosso, S., Graiff, L., Granata, S., Monaco, C., & Meneghello, R. (2024). A review of recent literature on the handling of anterior resin-bonded cantilever restorations. *Journal of Current Research in Oral Surgery, 4*(1), 1–8. doi:10.51847/JcU1FD46Qw

Dobbss, L. B., Medici, L. O., Peres, L. E. P., Pino-Nunes, L. E., Rumjanek, V. M., Façanha, A. R., & Canellas, L. P. (2007). Changes in root development of Arabidopsis promoted by organic matter from oxisols. *Annals of Applied Biology, 151*(2), 199–211. doi:10.1111/j.1744-7348.2007.00166.x

Duan, G. L., Yang, Y. P., Yi, X. Y., & Zhu, Y. G. (2024). The association of the biogeochemical processes between arsenic and organic substances in paddy soils. In *Arsenic in the environment: Bridging science to practice for sustainable development, As2021* (pp. 173–174). CRC Press. doi:10.1201/9781003317395-73

Elango, R., & Govindaraju, L. (2025). In vitro evaluation of Kedo Sdf gel effect on the micro-hardness of natural carious dentin. *Annals of Dental Specialty, 13*(2), 12–14. doi:10.51847/fQknFGnize

Farley, K. A., Kelly, E. F., & Hofstede, R. G. (2004). Soil organic carbon and water retention after conversion of grasslands to pine plantations in the Ecuadorian Andes. *Ecosystems, 7*, 729–739. doi:10.1007/s10021-004-0047-5

Federal Agency for Technical Regulation and Metrology. (2021). *GOST 26213-2021: Soils. Methods for determination of organic matter*. FGBU "RST".

Hao, C., Fang, L., & Lin, Z. (2025). Autonomous AI agent for QSAR modeling with dataset curation, descriptor selection, and domain assessment. *Pharmacophore, 16*(4), 11–21. doi:10.51847/Bhyi6RjARa

Holliger, C., Gaspard, S., Glod, G., Heijman, C., Schumacher, W., Schwarzenbach, R. P., & Vazquez, F. (1997). Contaminated environments in the subsurface and bioremediation: Organic contaminants. *FEMS Microbiology Reviews, 20*(3–4), 517–523. doi.:10.1111/j.1574-6976.1997.tb00334.x

Huang, L. M., Zhang, X. H., Shao, M. A., Rossiter, D., & Zhang, G. L. (2016). Pedogenesis significantly decreases the stability of water-dispersible soil colloids in a humid tropical region. *Geoderma, 274*, 45–53. doi:10.1016/j.geoderma.2016.04.005

Huber, M. A., Bauer, L. S., Gruber, F. K., & Müller, E. W. (2025). Outcomes of everolimus combined with exemestane in HR-positive metastatic breast cancer after CDK4/6 inhibitor exposure. *Archives of International Journal of Cancer and Allied Sciences, 5*(2), 44–50. doi:10.51847/sJNxEiRZXn

Jannath, A., Sivapragasam, S., Viswanathan, K., & Sundaram, R. (2024). Intentional replantation with simultaneous periapical surgery: A case report with one year of follow-up. *Annals of Dental Specialty, 12*(3), 23–27. doi:10.51847/JIs54FRstW

Kajanova, J., & Badrov, A. (2024). Medical students' perspectives on trust in medical AI: A quantitative comparative study. *Asian Journal of Ethics and Health Medicine, 4*, 44–57. doi:10.51847/36mpdZ9AZ8

Kassenova, Z., Iskakov, Y., Yermagambet, B., Kapsalyamov, B., Saulebekova, M., Imbayeva, D., Kazankapova, M., & Nasyrova, D. (2024). Effectiveness of oil-contaminated soil reclamation with humic preparations. *International Journal of Agriculture and Biosciences, 13*(3), 474–487. doi:10.47278/journal.ijab/2024.154

Kassenova, Z., Yermagambet, B., Kazankapova, M., Tastambek, K., Akimbekov, N., Kozhakhmetova, M., Kamenov, B., Nussipov, D., Altynbay, N., Sherelkhan, D., Slamiya, M., & Imbayeva, D. (2025). Bioremediation of oil-polluted soils using humic substances and microorganisms. *ES Food & Agroforestry, 19*, 1310. doi:10.30919/esfaf1310

Kondrashina, V., Strijakova, E., Zinnatshina, L., Bocharnikova, E., & Vasilyeva, G. (2018). Influence of activated carbon and other additives on bioremediation rate and characteristics of petroleum-contaminated soils. *Soil Science, 183*(4), 150–158. doi:10.1097/SS.0000000000000234

Kowalski, T. W., Reis, L. B., Andreis, T. F., Ashton-Prolla, P., & Rosset, C. (2024). Rare co-occurrence of two mutational variants in NF1: Molecular testing reveals diagnostic surprises. *Journal of Medical Sciences and Interdisciplinary Research, 4*(2), 20–29. doi:10.51847/H2qQlZTYO7

Kuzyakov, Yu. Ya., Semenenko, K. A., & Zorov, N. B. (1990). *Metody spektralnogo analiza: Ucheb. posobie [Spectral analysis methods: A manual].* Izd-vo MGU.

Kwatra, D., Venugopal, A., & Anant, S. (2024). Studying the efficacy of tolmetin radiosensitizing effect in radiotherapy treatment on human clonal cancer cells. *Bulletin of Pioneer Research in Medical and Clinical Sciences, 4*(2), 22–28. doi:10.51847/Uuhjk0fMC8

Li, M., Hu, H., He, X., Jia, J., Drosos, M., Wang, G., & Xi, B. (2019). Organic carbon sequestration in soil humic substances as affected by application of different nitrogen fertilizers in a vegetable-rotation cropping system. *Journal of Agricultural and Food Chemistry, 67*(11), 3106–3113. doi:10.1021/acs.jafc.8b07114

Manucharova, N. A., Pozdnyakov, L. A., Vlasova, A. P., Yanovich, A. S., Ksenofontova, N. A., Kovalenko, M. A., Stepanov, P. Y., Gennadiev, A. N., Golovchenko, A. V., & Stepanov, A. L. (2021). Metabolically active prokaryotic complex in grassland and forests' sod-podzol under polycyclic aromatic hydrocarbon influence. *Forests, 12*(8), 1103. doi:10.3390/f12081103

Mishra, N., Dadhich, A., Vande, A. V., Saluja, H., Shah, S., & Mishra, M. (2025). A comparative assessment of topical 5-fluorouracil and modified Carnoy's solution for the treatment of odontogenic keratocyst. *Journal of Current Research in Oral Surgery, 5*(1), 11–16. doi:10.51847/OrVjjlmrxW

Mora, V., Bacaicoa, E., Baigorri, R., Zamarreno, A. M., & García-Mina, J. M. (2014). NO and IAA key regulators in the shoot growth-promoting action of humic acid in *Cucumis sativus* L. *Journal of Plant Growth Regulation, 33*(2), 430–439. doi:10.1007/s00344-013-9394-9

Moreno-Jiménez, E., Esteban, E., & Peñalosa, J. M. (2011). The fate of arsenic in soil-plant systems. *Reviews of*

Environmental Contamination and Toxicology, 215, 1–37. doi:10.1007/978-1-4614-1463-6_1

Morgan, A. L., Foster, D. K., & Collins, I. J. (2025). Disparities in HER2-targeted therapy adoption and survival impact in metastatic HR−/HER2+ breast cancer: NCDB cohort study. *Asian Journal of Current Research in Clinical Cancer, 5*(2), 1–11. doi:10.51847/AZI4JURGlQ

Nagesh, D., Lam Ip, C. Y. T., Li, K., Wong, H. S. L., & Chai, J. Y. H. (2025). Navigating support networks: A Somali woman's experience of social alignment to overcome isolation during pregnancy and early motherhood. *International Journal of Social Psychology Aspects of Healthcare, 5*, 35–48. doi:10.51847/iJoPhqpXaV

Nguyen, T. T., Dinh, V. T., & Vu, L. H. (2025). An integrated FAHP–TOPSIS approach for evaluating and prioritizing medical tourism service types in Vietnam. *Journal of Organizational Behavior Research, 10*(2), 20–31. doi:10.51847/lnWweTmy0d

Novak, H., & Jelic, P. (2025). Comparing self-learning skill stations and instructor-led courses for cardiopulmonary resuscitation skill retention among hospital nurses: A randomized controlled trial. *Journal of Integrative Nursing and Palliative Care, 6*(2), 185–191. doi:10.51847/MFRNxbMHX7

Novak, T. J., & Dvorak, P. M. (2025). A spatiotemporal neural network framework for EEG-based emotion recognition in depression assessment. *Journal of Medical Sciences and Interdisciplinary Research, 5*(2), 24–38. doi:10.51847/A2pBOYHJW1

Olaetxea, M., De Hita, D., Garcia, C. A., Fuentes, M., Baigorri, R., Mora, V., Garnica, M., Urrutia, O., Erro, J., Zamarreño, A. M., Berbara, R. L., & Garcia-Mina, J. M. (2018). Hypothetical framework integrating the main mechanisms involved in the promoting action of rhizospheric humic substances on plant root and shoot growth. *Applied Soil Ecology, 123*, 521–537. doi:10.1016/j.apsoil.2017.06.007

Qiao, J., Li, X., Li, F., Liu, T., Young, L. Y., Huang, W., Sun, K., Tong, H., & Hu, M. (2019). Humic substances facilitate arsenic reduction and release in flooded paddy soil. *Environmental Science & Technology, 53*(9), 5034–5042. doi:10.1021/acs.est.8b06333

Salem, H. M., Watanabe, S., & Chang, A. H. (2025). Ethical concerns in managing anorexia nervosa: A content analysis of ethics consultation records. *Asian Journal of Ethics and Health Medicine, 5*, 25–35. doi:10.51847/oHEI6FgL3V

Santos, J. A., Nunes, L. A., Melo, W. J., & Araújo, A. S. (2011). Tannery sludge compost amendment rates on soil microbial biomass of two different soils. *European Journal of Soil Biology, 47*(2), 146–151. doi:10.1016/j.ejsobi.2011.01.002

Shadrin, D., Pukalchik, M., Kovaleva, E., & Fedorov, M. (2020). Artificial intelligence models to predict acute phytotoxicity in petroleum-contaminated soils. *Ecotoxicology and Environmental Safety, 194*, 110410. doi:10.1016/j.ecoenv.2020.110410

State Committee of the USSR for Standards. (1985). *GOST 26483-85 Soils. Preparation of salt extract and determination of its pH by the CINAO method*. Izdatel'stvo Standartov.

Svensson, A., & Lindberg, E. (2026). Explainable AI for pediatric dosing error prediction using prescription text and weight-based rules. *Pharmacophore, 17*(2), 1–11. doi:10.51847/v5wAxGMQYm

Taran, D. O., Zhdanova, G. O., Saksonov, M. N., Barchatova, O. A., Bybin, V. A., & Stom, D. I. (2013). The effect of humic substances on test objects. *Acta Biomedica Scientifica, 6*(94), 164–168.

Trofimov, S. Ya., Kovaleva, E. I., Avetov, N. A., & Tolpeshta, I. I. (2023). Studies of oil-contaminated soils and prospective approaches for their remediation. *Moscow University Soil Science Bulletin, 78*(4), 387–395. doi:10.3103/S0147687423040099

Vaccari, D. A., Powers, S. M., & Liu, X. (2019). Demand-driven model for global phosphate rock suggests paths for phosphorus sustainability. *Environmental Science & Technology, 53*(17), 10417–10425. doi:10.1021/acs.est.9b02464

Vasilyeva, G. K., Kondrashina, V. S., Strijakova, E. R., & Pinsky, D. L. (2022). Express-phytotest for choosing conditions and following the process of soil remediation. *Environmental Geochemistry and Health, 44*(2), 433–445. doi:10.1007/s10653-020-00727-8

Vikram, N., Sagar, A., Gangwar, C., Husain, R., & Kewat, R. N. (2022). Properties of humic acid substances and their effect on soil quality and plant health. IntechOpen. doi.:10.5772/intechopen.105803

Viruel, E., Lucca, M. E., & Sineriz, F. (2011). Plant growth promotion traits of phosphobacteria isolated from Puna, Argentina. *Archives of Microbiology, 193*, 489–496. doi:10.1007/s00203-011-0692-y

Wang, L., Zhang, Y., Xu, C., Dong, Q., Lv, Y., Wang, M., Su, X., Jiang, H., Xu, Y., Sun, F., Yin, X., & Zhai, R. (2022). Effects of humic acid fertilizers on arsenic and mercury speciation and enzyme activities in soil. *Research Square*. doi:10.21203/rs.3.rs-2274116/v1

Xu, H., Yan, Z., Cai, H., Yu, G., Yang, L., & Jiang, H. (2013). Heterogeneity in metal binding by individual fluorescent components in a eutrophic algae-rich lake. *Ecotoxicology and Environmental Safety, 98*, 266–272. doi:10.1016/j.ecoenv.2013.09.008

Xue, Q., Ran, Y., Tan, Y., Peacock, C. L., & Du, H. (2019). Arsenite and arsenate binding to ferrihydrite organo-mineral coprecipitate: Implications for arsenic mobility and fate in natural environments. *Chemosphere, 224*, 103–110. doi:10.1016/j.chemosphere.2019.02.118

Yang, F., & Antonietti, M. (2020). The sleeping giant: A polymer view on humic matter in synthesis and applications. *Progress in Polymer Science, 100*, 101182. doi:10.1016/j.progpolymsci.2019.101182

Yang, F., Tang, C., & Antonietti, M. (2021). Natural and artificial humic substances to manage minerals, ions, water, and soil microorganisms. *Chemical Society Reviews, 50*(10), 6221–6239. doi:10.1039/D0CS01363C

Yang, F., Zhang, S., Cheng, K., & Antonietti, M. (2019). A hydrothermal process to turn waste biomass into artificial fulvic and humic acids for soil remediation. *Science of the Total Environment, 686*, 1140–1151. doi:10.1016/j.scitotenv.2019.06.045

Yermagambet, B. T., Kasenova, Z. M., Nurgaliev, N. U., & Kazankapova, M. K. (2021). *Patent of the Republic of Kazakhstan for invention No. 35020: Method for obtaining*

humic substances from oxidized weathered and brown coals. LLP SPO "Kaztechnougol."

Zairkhanova, L. N., Eremina, A. S., Burkhanov, R. R., Bersanova, M. M., Agerzhanokova, S. Z., Muskhadzhieva, F. A., Ataeva, A. I., & Esyunin, V. V. (2024). Investigation of the effectiveness of silver-containing drugs for the treatment of tuberculosis in the respiratory system. *Journal of Advanced Pharmacy Education and Research, 14*(3), 31–35. doi:10.51847/zhfsdGkmQi

Zhu, J., Li, M., & Whelan, M. (2018). Phosphorus activators contribute to legacy phosphorus availability in agricultural soils: A review. *Science of the Total Environment, 612*, 522–537. doi:10.1016/j.scitotenv.2017.08.095